

Unconfirmed Detection of a Transit of HD 80606b

E. Garcia-Melendo¹ & P. R. McCullough²

egarcia@foed.org

ABSTRACT

We report a times series of B-band photometric observations initiated on the eve of Valentine’s day, February 14, 2009, at the anticipated time of a transit of the extrasolar planet HD 80606b. A transit model favored by the data has minimum light of 0.990 times the nominal brightness of HD 80606. The heliocentric Julian date (HJD) of the model’s minimum light is 2454876.33, which combined with the orbital period $P = 111.4277 \pm 0.0032$ days, longitude of periastron, $\omega = 300.4977 \pm 0.0045$ degrees, and time of mid-secondary eclipse HJD 2454424.736 ± 0.003 (Laughlin et al. 2009), refines the eccentricity, $e = 0.9337^{+0.0012}_{-0.0004}$, and the inclination, $i = 89.26^{+0.24}_{-0.04}$ degrees. The duration of the model transit is 0.47 days, and its four contacts occur at HJD 2454876 plus 0.10, 0.24, 0.42, and 0.57 days. We observed only the last two contacts, not the first two. We obtained “control” time series of HD 80606 on subsequent nights; as expected, the “controls” do not exhibit transit-like features. We caution that 1) the transit has not been confirmed independently; 2) we did not observe the transit’s ingress; 3) consequently, we cannot reliably measure the relative sizes of the planet and its star in a model-independent manner, and 4) hence, the other values derived herein are also model dependent.

Subject headings: binaries: eclipsing – planetary systems – stars: individual (HD 80606) – techniques: photometric

¹Esteve Duran Observatory Foundation, 08553 Seva, Spain

²Space Telescope Science Institute, 3700 San Martin Dr., Baltimore MD 21218, USA

1. Introduction

HD 80606b is a gaseous giant planet, four times the mass of Jupiter, in an eccentric ($e = 0.93$) 111-day orbit about the G5V star HD 80606 (Naef et al. 2001). HD 80607, a physical companion to HD 80606 (Naef et al. 2001), provides a convenient comparison star for differential photometry of HD 80606, because the two have similar brightnesses, colors, and are separated by only $\sim 20''$. Laughlin et al. (2009) demonstrated with *Spitzer* IRAC photometry at $8\text{-}\mu\text{m}$ that the planet HD 80606b passes behind its host star and estimated a 15% probability that HD 80606b passes in front of its star also. At www.oklo.org, Laughlin encouraged a global campaign of observations of HD 80606b near the anticipated time of transit.

Figure 1 illustrates the Earth as it would appear from HD 80606 at the times of mid-transit for the transit reported here and the next three transits. Such diagrams are useful for planning observations of synoptic events with periods much longer than a month, because the location of the observatory on Earth is of primary importance. Figure 1 also tacitly illustrates a benefit of observing from above the Earth’s bright atmosphere for meeting a schedule of infrequent synoptic events, especially events requiring uninterrupted time series of many hours.

2. Observations

We observed the pair of stars HD 80606/7 with the 0.6-m diameter Cassegrain telescope of the Esteve Duran Observatory. The camera is a ST-9XE model manufactured by the Santa Barbara Imaging Group. For all of the observations reported here, we used an Optec B band filter. The CCD has 512 pixels by 512 pixels; each pixel is $20\ \mu\text{m} \times 20\ \mu\text{m}$, or $1''.27 \times 1''.27$. Image were corrected with dark images and flat fields. Individual exposures were 10 seconds, obtained at a cadence of 12.1 seconds. The B filter enabled keeping the shutter open for a large fraction (83%) of the observing time while avoiding saturation from the bright stars. Per pixel, the peak of the PSFs was ~ 5000 DN, and the background ~ 70 DN. The telescope was focused to $\sim 5''$ FWHM, in order to prevented blending of the wings of the point spread functions (PSFs) of the target, HD 80606, and the comparison star, HD 80607.

3. Analysis

Because the angular separation of the two stars was ~ 4 times their PSF’s FWHM, we used conventional aperture photometry. Results do not depend significantly on aperture

size; the results reported here used a circular aperture of radius 7 pixels ($\sim 9''$). The small angular separation, similar color indices between the target star and the comparison star, and moderate range of airmass (1.0 to 1.7) permitted differential photometry without extinction and color corrections. The nightly photometric averages of out-of-transit time series differ by $\sim 0.1\%$ for four different nights and are consistent with negligible corrections. The night of the transit, the sky was clear all night; on three subsequent nights used to obtain “controls,” the clarity was substantially more variable, and yet the differential photometry remained similar in quality to that of the night of the transit, 0.64% r.m.s. per 10-sec exposure, and 0.14% r.m.s. per 5-min average (Figure 2).

The stars drifted ~ 60 pixels across the CCD during the first half of the night of the transit; hereafter we refer to that drift as the “nominal” trajectory. While we were initially concerned that the drift may have created the photometric change which we interpret as the egress of HD 209458b, we have observational evidence that the position drift is unlikely to be responsible for the gradual rise in the light curve from HJD 2454876.42 to 2454876.57. After a 17-min gap in observations required during meridian crossing (from HJD 2454876.531 to 2454876.543), the stars were re-acquired again near their positions at which they began the night. Although the positions have a discontinuity across the gap of 50 pixels, the differential photometry does not change across the gap. Indeed, zero offset has been applied to match the photometry across the gaps at the meridian in any of the light curves. Serendipitously the vector offset from HD 80606 to HD 80607 is similar in direction but $\sim 1/4$ as large as the 60-pixel length of the nominal trajectory; consequently, if the *differential* photometry was affected by $\sim 1\%$ due to incorrect calibration (e.g. due to a gradient in either vignetting or quantum efficiency of the CCD), the amplitude of the erroneous calibration across the *entire* trajectory would need to be $\sim 4\%$. The B-band flat field is very uniform; along the nominal trajectory, there is a single feature, a ring from a de-focused dust speck, with a 4-pixel inner radius and an 8-pixel outer radius, and $\lesssim 0.8\%$ fainter than nominal within the two radii. The flat field spatial variation is 0.6% r.m.s. on a per-pixel basis, with a best-fitting gradient that amounts to 0.4% from end-to-end across the nominal trajectory. The latter is ~ 10 times smaller than our estimate ($\sim 4\%$) of the erroneous calibration that would be required to explain the $\sim 1\%$ variation in the light curve during egress. On the final “control” night, we purposefully induced a drift of the stars’ positions on the CCD along a trajectory similar in initial position and vector direction to the nominal trajectory. Even with an induced drift of more than twice the angle of the nominal trajectory, we detected no significant correlation of differential photometry with image position on the final “control” night. We conclude that the transit-like variation in the light curve is not an instrumental artifact.

We model the observed transit light curve (Figure 3) using the algorithms of Mandel & Agol (2002). A required input to the latter algorithms is the time-dependent projected

separation of the center of the planet from the center of the star in units of the radius of the star. For the latter, we use Eq. 5.63 of Hilditch (2001) for eccentric orbits. For simplicity, we interpolate and fix the quadratic limb darkening coefficients, $\gamma_1 = 0.711$ and $\gamma_2 = 0.124$, from Claret (2000) as appropriate for the B filter bandpass, and for HD 80606’s spectroscopic gravity, effective temperature, and metallicity ($\log g = 4.50 \pm 0.20$, $T_{eff} = 5645 \pm 45$, and $[Fe/H] = +0.43 \pm 0.06$; Naef et al. 2001). Also from Naef et al. (2001), we adopt the semi-major axis $a = 0.469$ AU, or equivalently HD 80606’s stellar mass $M_* = 0.90M_\odot$. We adopt the following orbital parameters from Laughlin et al. (2009): the orbital period $P = 111.4277 \pm 0.0032$ days; the longitude of periastron, $\omega = 300.4977 \pm 0.0045$ degrees, the heliocentric Julian date of periastron passage, $T_{peri} = 2454424.86$, and the radius of the planet, $R_p = 1.1R_J$. We adopt a stellar radius, $R_* = 1.0R_\odot$; in order to model the light curve we use the dimensionless semi-major axis $a/R_* = 100$, and the ratio of planetary and stellar radii, $R_p/R_* = 0.11$.

There are two remaining parameters required in order to model the light curve: the eccentricity and the orbital inclination. Because we only observed egress, the latter two parameters are correlated (Figure 4), and the uncertainties of the derived inclination are asymmetric. For small deviations about their nominal values, $e = 0.9337$ and $i = 89.26^\circ$, the eccentricity may be increased by δe in order to accommodate an increase in the orbital inclination of $\sim 200^\circ \delta e$. Increasing the eccentricity by 0.0001 shifts the transit earlier by 0.01 day. With the constraint of the observed time of egress, increasing the orbital inclination by 0.1° must be accommodated by shifting the transit mid-point earlier by 0.05 day, i.e. increasing the eccentricity by 0.0005. The eccentricity derived from fitting the transit egress, essentially determining the elapsed time from the secondary eclipse to the transit, is $e = 0.9337^{+0.0012}_{-0.0004}$, which is consistent with the value and uncertainty estimated from radial velocities, $e = 0.9327 \pm 0.0023$ (Laughlin et al. 2009). The large asymmetry of the uncertainty is caused by the one-sided constraint of having observed only egress.

Figure 3 shows four models. The nominal model, which the data favor, has eccentricity $e = 0.9337$ and inclination $i = 89.26^\circ$, and reduced chi-squared $\chi_\nu^2 = 2.5$. The associated minimum separation during transit of the centers of the planet and the star, $z_{min} = 0.85R_*$. For comparison, Figure 3 shows three other models with (e, i, χ_ν^2) triplets: $(0.9333, 89.22^\circ, 3.0)$, $(0.9349, 89.50^\circ, 3.0)$, and $(0.9337, 90^\circ, 3.6)$. If $R_p/R_* = 0.11$ as we have assumed, the central-transit model, is incompatible with our observations; the other two are marginally acceptable. However, if the planet-to-star size ratio, $R_p/R_* = 0.09$, for example, our data *prefer* the central-transit model. From our egress data alone, we cannot distinguish between a model with a smaller planet, larger inclination, and larger eccentricity from another model with a larger planet, smaller inclination, and smaller eccentricity.

The heliocentric Julian date of minimum light of our adopted transit model is

$$t_{m.l.} = 2454876.33 + P \times E, \quad (1)$$

where E is an integer. The duration of the model transit is 0.47 days; the predicted heliocentric Julian dates of the four contacts are 2454876 plus 0.10, 0.24, 0.42, and 0.57 days.

We are aware of a few null-detections of transits of HD 80606b (e.g. www.oklo.org). We are not aware of any that directly conflict with the observations reported here either because they do not overlap in time or because the photometric differences appear to be statistically insignificant. If our model is correct, this transit of HD 80606b finished before it was visible to North American observers. Observations of Gregor Srdoc (p.c.) from Croatia for the interval from HJD 2454876.22 to 2454876.66, which includes contacts 2, 3, and 4 of the model transit discussed here, were compromised by clouds and blending of the de-focused images of HD 80606 and HD 80607 into one photometric aperture, which would dilute the $\sim 1.0\%$ depth of the transit reported here to a depth of $\sim 0.5\%$.

If independent observations confirm this transit, they also may better constrain the eccentricity and the inclination. For a near-grazing transit of a star with nominal limb darkening, the transit’s depth should be slightly greater at longer wavelengths. Comparison of our B-band data with data obtained through a redder filter could confirm the large impact parameter and eliminate degeneracies inherent to single-color transit light curves (see e.g. the analysis of TrES-3 by O’Donovan et al. 2007). The wiggles at the beginning (also bottom) of the light curve may be either due to poorer calibration at large airmass, or due to nonuniformities (spots) on the surface of the star, HD 80606.

4. Summary

We report an unconfirmed detection of a transit of HD 80606b observed in B band. The transit depth and egress duration are consistent with expectations for an assumed planetary-to-stellar size ratio, $R_p/R_* = 0.11$, and a projected, closest-approach impact parameter of 0.85 stellar radii. We caution that 1) the transit has not been confirmed independently; 2) we did not observe the transit’s ingress; 3) in our modeling we assumed a theoretical value for the relative sizes of the planet and its star; and 4) hence, the other values derived herein are also model dependent.

We report these observations in the hope that they may be confirmed or refuted by additional observations. Especially useful could be observations from Asia, from which ingress of this transit would have been visible.

P. R. M. is funded primarily by NASA Origins of Solar Systems grant NNG06GG92G.

REFERENCES

Claret, A. 2000, *A&A*, 363, 1081

Hilditch, R. W. 2001, *An Introduction to Close Binary Stars*, by R. W. Hilditch, pp. 392. ISBN 0521241065. Cambridge, UK: Cambridge University Press

Laughlin, G., Deming, D., Langton, J., Kasen, D., Vogt, S., Butler, P., Rivera, E., & Meschiari, S. 2009, *Nature*, 457, 562

Mandel, K., & Agol, E. 2002, *ApJ*, 580, L171

Naef, D., et al. 2001, *A&A*, 375, L27

O’Donovan, F. T., et al. 2007, *ApJ*, 663, L37

Table 1. Time-Series Photometry

HJD	Mag
2454876.33378	-0.1409
2454876.33392	-0.1445
2454876.33407	-0.1537
2454876.33421	-0.1540
2454876.33436	-0.1497

Column 1 is the mid-exposure heliocentric Julian day.
Column 2 is the differential B-band magnitude of HD 80606
with respect to the comparison star HD 80607.
The complete table is available online.

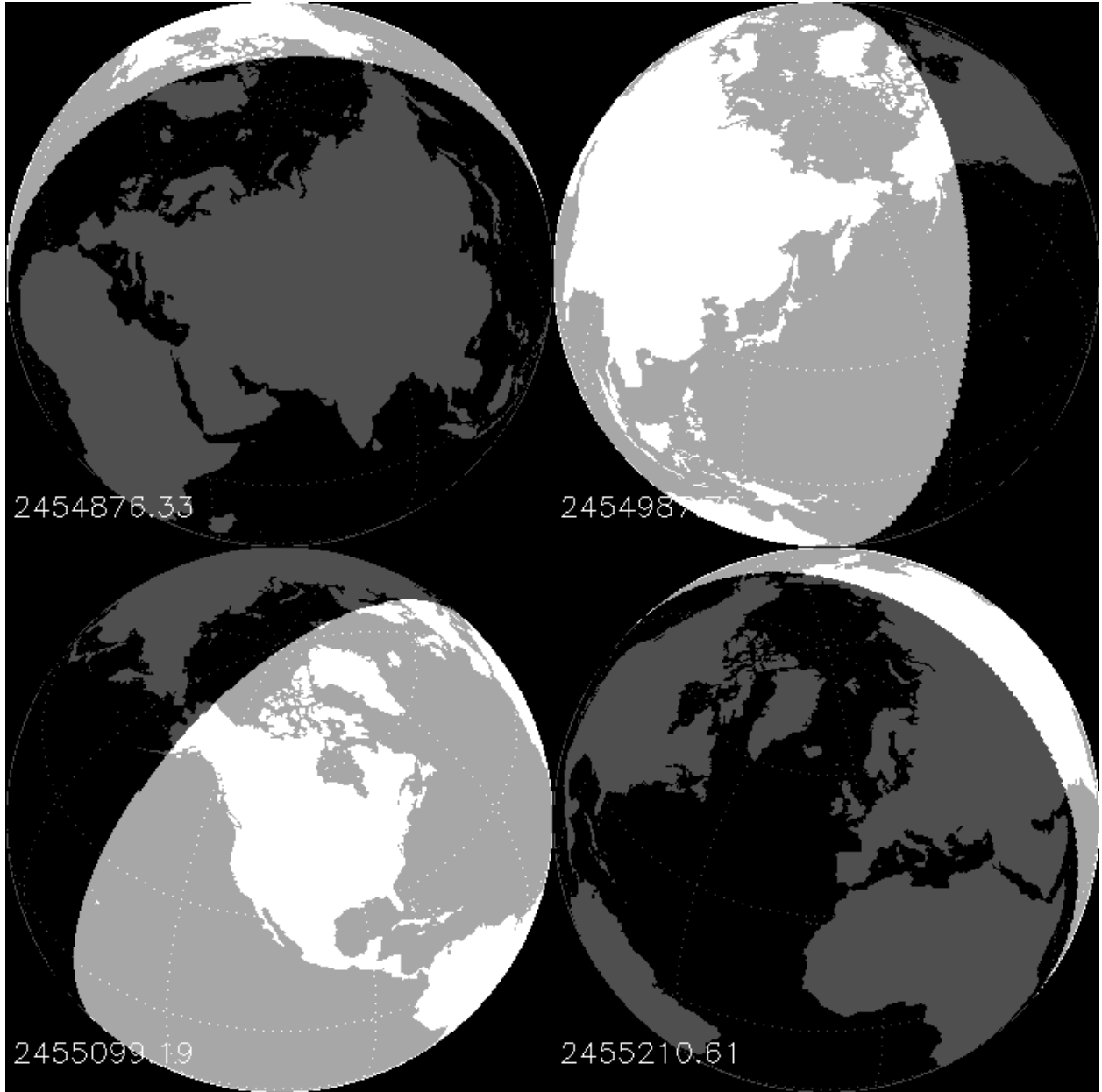


Fig. 1.— Views of Earth from HD 80606b at mid-transit. The predicted HJD of minimum light is labeled. Areas in which the Sun is above the local horizon are brighter. The next two opportunities to observe a transit of HD 80606b from the surface of the Earth (upper right and lower left) are not as favorable in terms of daylight and local airmass as the one reported here (upper left) or the one 334 days later (lower right).

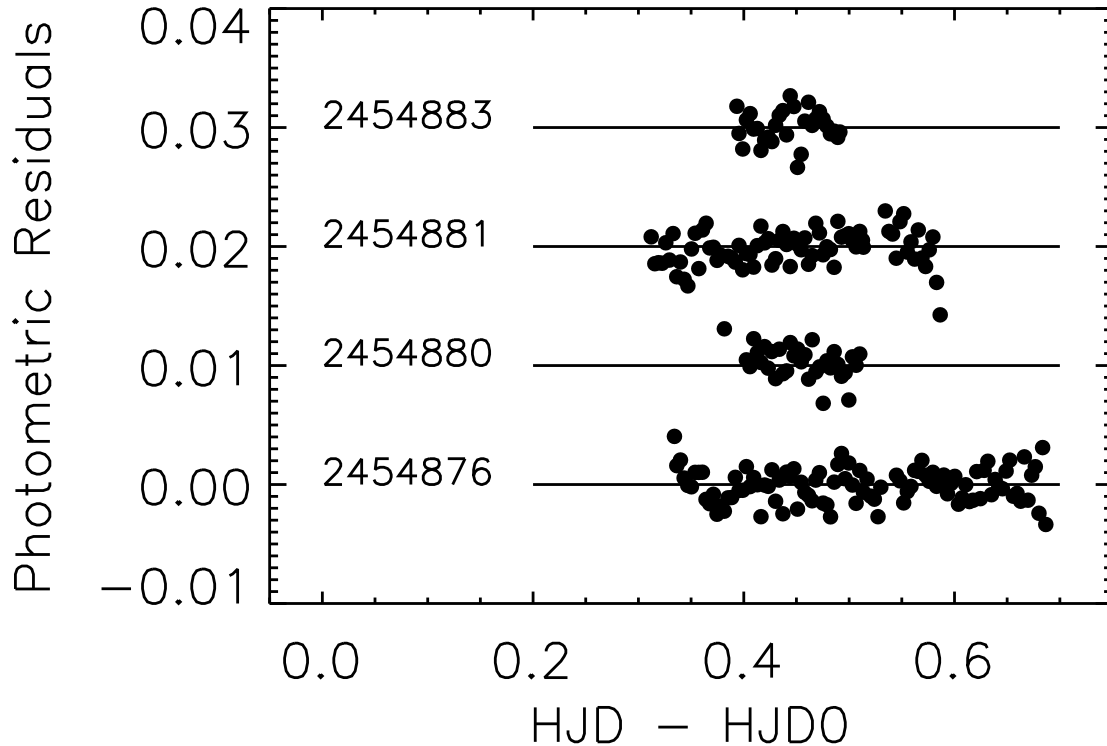


Fig. 2.— Photometric residuals. Differential photometric residuals of HD 80606 with respect to HD 80607 on four nights are shown. The four times series were obtained and analyzed in an identical manner. The original observations have been averaged into 5-min bins. The residuals from the night of the transit ($HJD_0 = 2454876$) are with respect to the nominal transit model (solid line of Figure 3). The others, the “controls,” are with respect to constant-brightness models on the dates indicated and have been shifted vertically for clarity. The values of HJD_0 are indicated to the left of each series. On this scale, the observed transit would extend from one horizontal line to another.

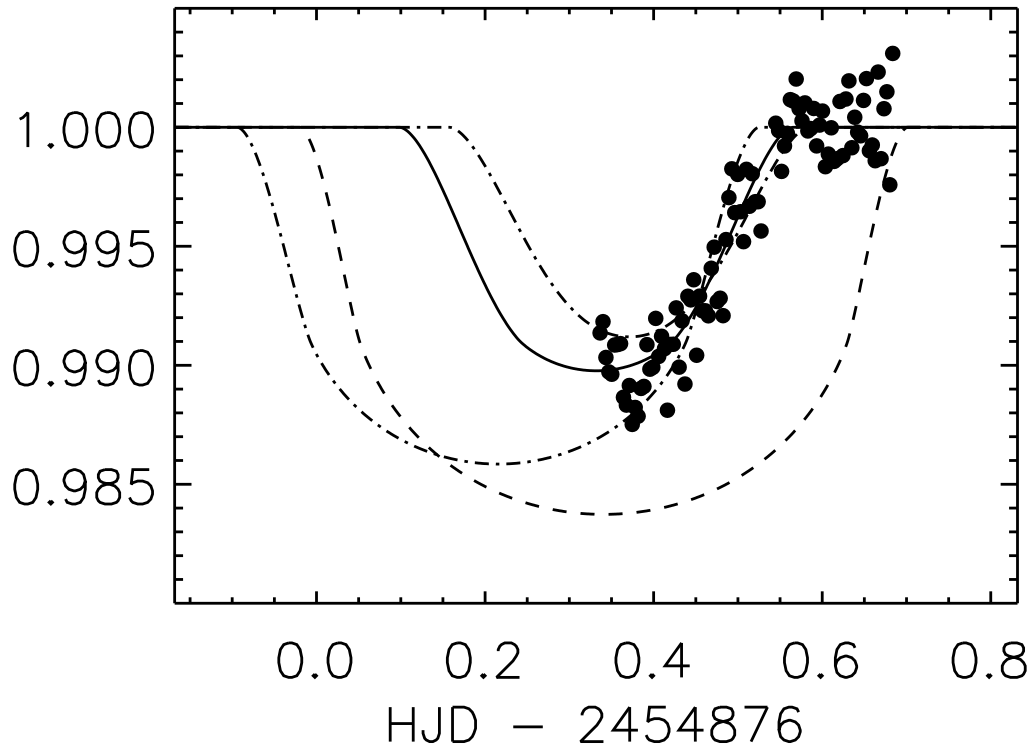


Fig. 3.— Egress of HD 80606b. Time-series B-band differential photometry of HD 80606, as observed with the 0.6-m telescope of the Esteve Duran Observatory during the February 13-14, 2009 transit of HD 80606b. The data from Table 1, averaged into 5-minute intervals (filled circles), and four models are shown: the nominal transit model described in the text (solid line), two marginally-acceptable models (dot-dashed lines), and a central-transit model (dashed line) for comparison. All four models assume $R_p/R_* = 0.11$.

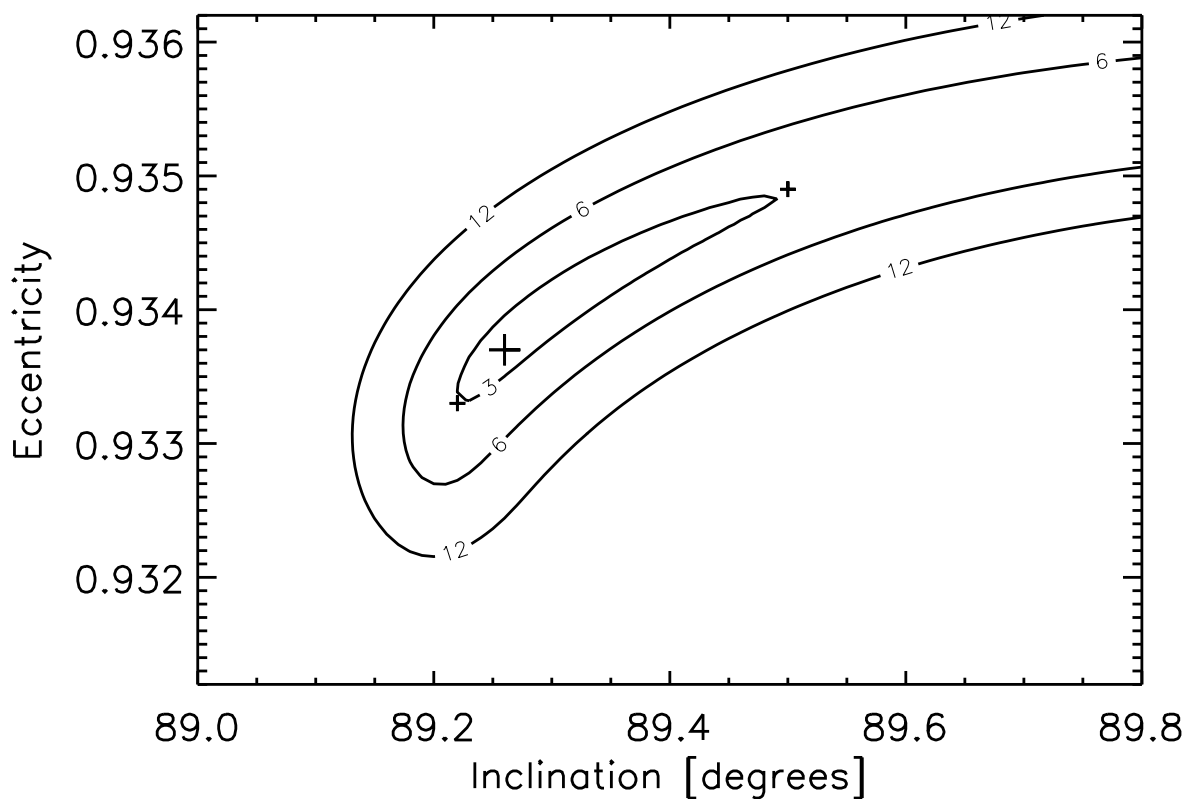


Fig. 4.— Contours of reduced chi-squared for the transit light curve (Figure 3). The large plus (+) symbol indicates the nominal parameters for eccentricity and inclination adopted in this work. The two smaller plus (+) symbols indicate the marginally-acceptable models also illustrated in Figure 3. As indicated by the contours and discussed in the text, deviations from the nominal value of inclination can be compensated with deviations in eccentricity.